J. Fluid Mech. (1975), *vol.* 68, *part* 3, *pp.* 567–575

Printed in Great Britain

Transition to turbulence in oscillating pipe flow

By P. MERKLI AND H. THOMANN

Institute of Aerodynamics, Swiss Federal Institute of Technology, Zurich

(Received 10 September 1973 and in revised form 25 February 1974)

Published results on transition in a Stokes layer indicate a wide range of transition Reynolds numbers. As thermal effects in a resonance tube (Merkli & Thomann 1975) depend on the state of the boundary layer, the transition Reynolds number was determined, and a critical Reynolds number $A_c \approx 400$ was found. The observations were made with hot wires and with flow visualization by means of smoke, and provide new details on turbulence in a Stokes layer. With this knowledge an explanation of the large discrepancies between some stability theories and the experiments is suggested. The main point is that turbulence occurs in the form of periodic bursts which are followed by *relaminarization* in the same cycle and do *not* lead to turbulent flow during the whole cycle.

A further, unexpected result of the present investigation is the discovery of vortex patterns superimposed on the normal laminar acoustic motion.

1. Introduction

During an investigation of thermal effects in a piston-driven resonance tube (Merkli 1973; Merkli & Thomann 1975) discrepancies between theory and experiment were noted for large oscillation amplitudes. There arises the question whether these differences are due to nonlinear effects or to turbulence in the boundary layer (Stokes layer) or both. Several papers concerning the stability of Stokes layers have been published (Li† 1954; Vincent† 1957; Collins† 1963; Sergeev† 1966; von Kerczek & Davis 1972; von Kerczek 1973; Pélissier† 1973; Daneshyar‡). All authors agree that transition is a local event, provided that the boundary-layer thickness $\delta = O((\nu/\omega)^{\frac{1}{2}})$ is small compared with other dimensions (e.g. the tube radius in our case). As long as this is true, transition is governed by the local Reynolds number based on δ, i.e.

$$Re_\delta = 2^{\frac{1}{2}}\hat{u}/(\nu\omega)^{\frac{1}{2}}$$

or, as in Sergeev's paper,

$$A = 2\hat{u}/(\nu\omega)^{\frac{1}{2}},$$

where ν = kinematic viscosity, ω = radian frequency and $\hat{u}$ = axial velocity amplitude. However, the numerical values for the critical Reynolds number

† While we used air ($\gamma = 1{\cdot}4$) in our experiments, these investigators worked with water ($\gamma = 1{\cdot}0$). Nevertheless, the different experiments may be compared, because the present stability theories consider the axial velocity component u only. In gas flows, for a first approximation, only the radial velocity v depends on γ while u is still independent of it. The main effect of setting $\gamma = 1$ is to decouple the energy equation from the flow field.

‡ See footnote in paper by Scarton & Rouleau, *J. Fluid Mech.* vol. 58, 1973, p. 596.

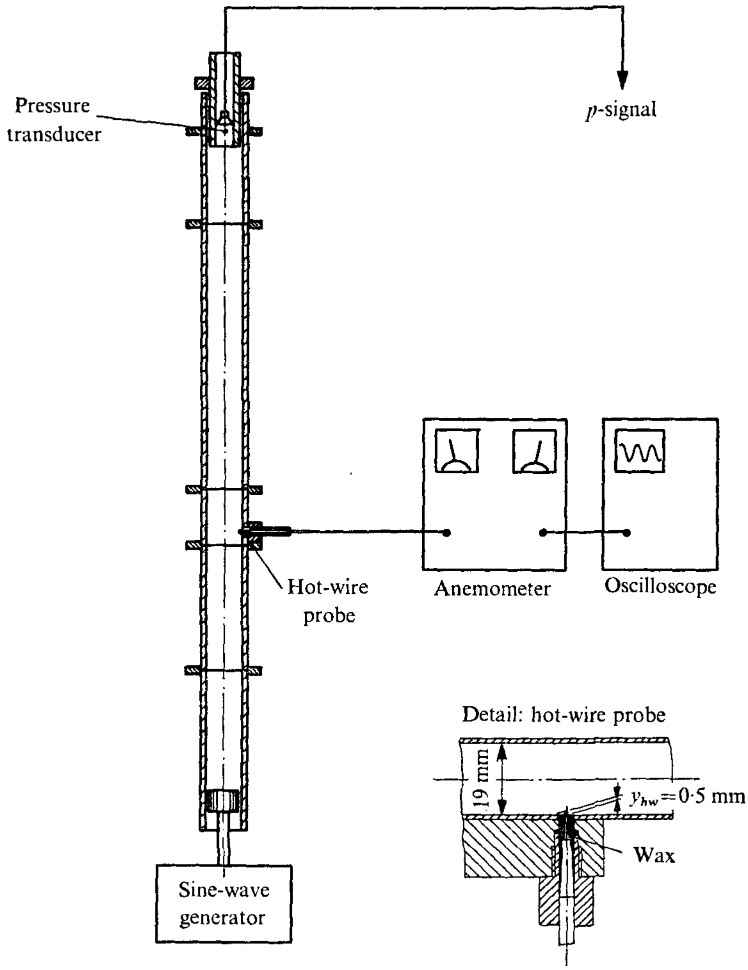

FIGURE 1(*a*). For legend see facing page.

quoted in the literature differ widely. From experiments with fluid oscillations in pipes Sergeev (1966) gives a value of A_c of 700. Von Kerczek & Davis (1972), on the basis of theoretical work using the energy method, state that turbulence will not occur for $Re_\delta < 19$, corresponding to an A_c of 27, but von Kerczek (1973), as a result of a linearized stability analysis in which integration is carried out over a full cycle, states that there probably does not exist any Reynolds number above which turbulence has to appear. In view of the uncertainties in the published experimental and theoretical results, it was decided to conduct a series of experiments on transition. The information gained in this investigation seems to clarify the present situation. The main point is that there are two possible forms in which turbulence may occur.

(*a*) *Turbulent flow throughout* the whole cycle of oscillation.

(*b*) *Turbulent bursts* followed by *relaminarization* in the same cycle.

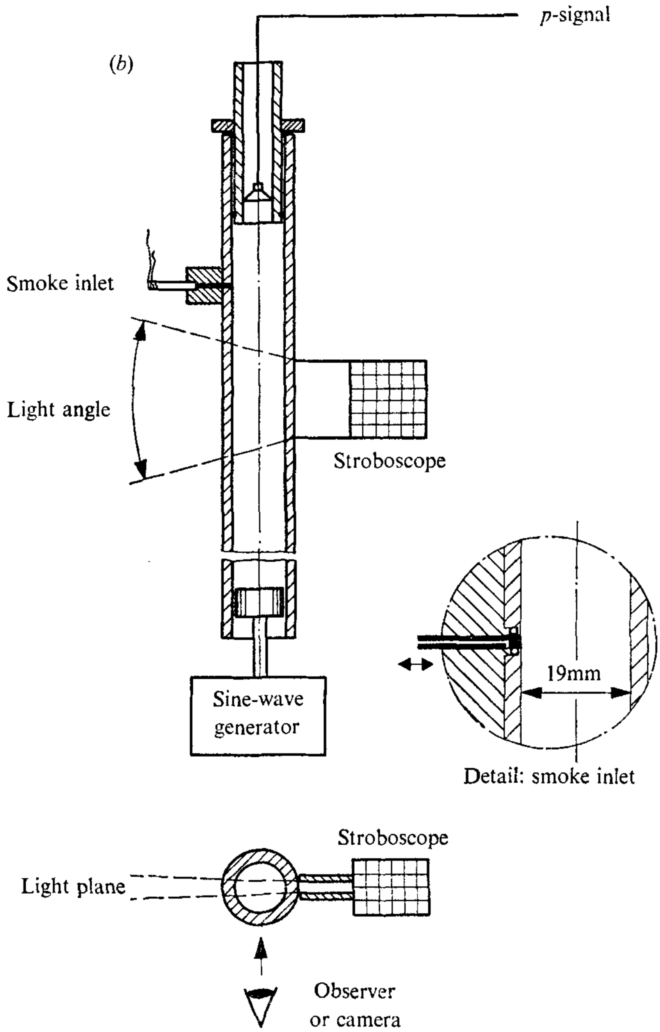

FIGURE 1. Experimental arrangement for (*a*) the hot-wire measurements and (*b*) the flow visualization.

In earlier experiments, these two cases were not distinguished, and it was assumed that the first one was appropriate. However, our hot-wire measurements indicate that the second one occurs. In the present work, transition was observed not only with hot wires but also by means of flow visualization with smoke. These experiments revealed, in addition, that vortex patterns exist along the tube wall which are too weak to be observed by normal pressure measurements.

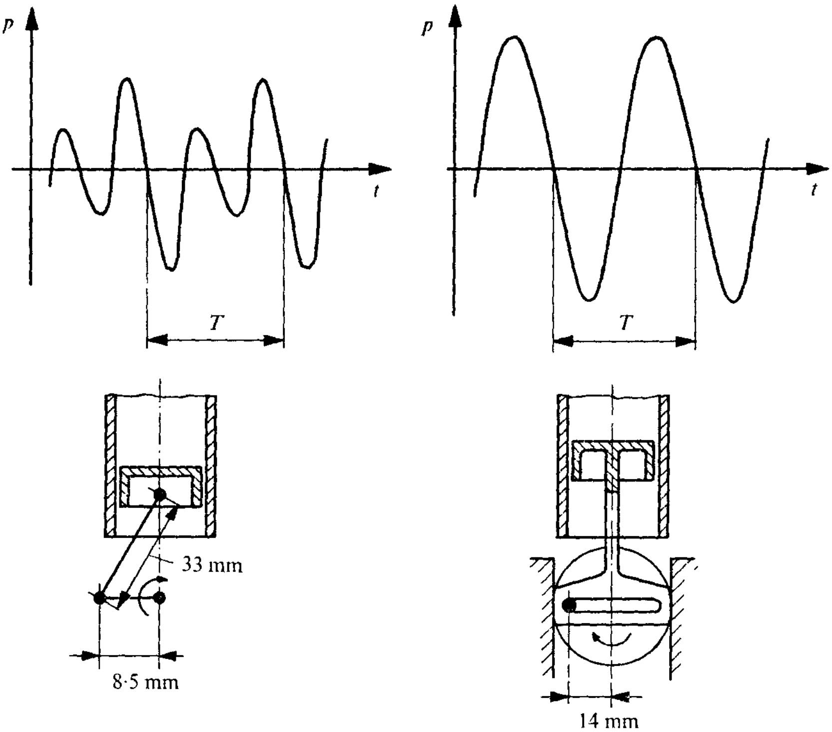

FIGURE 2. The pressure signals at the closed end of the tube ($L = 1{\cdot}4$ m) at half the resonance frequency ($f = 61$ Hz) for a normal crankshaft (amplitude $l = 8{\cdot}5$ mm) and for the mechanical sine-wave generator (amplitude $l = 14$ mm).

2. Experimental arrangement

Figures 1 (*a*) and (*b*) give a schematic survey of the experimental set-up. The tube is closed at one end by a shiftable end piece to set the tube length. It contains a pressure transducer (piezo-quartz)† whose signal allows determination of the oscillation frequency. The oscillations are driven by an oscillating piston at the other end of the tube. To have simple conditions, a special, lag-free, mechanical sine-wave generator was used to excite the motion of the gas column and precautions were taken to prevent transmission of vibrations of the driving mechanism to the tube. The amplitude of the piston could be chosen in the range of $2{\cdot}85 \leqslant l \leqslant 13{\cdot}8$ mm, and the frequency range was $0 \leqslant f \leqslant 130$ Hz. For the case where the piston is driven with a normal crankshaft, figure 2 illustrates the influence of higher harmonics when an overtone of the driving mechanism coincides with a resonance condition in the tube. This figure also gives an impression of the good quality of the sine-wave motion which was generated by the driving device used later.

If we excite the oscillations with a frequency too near the resonance frequency, travelling shocks appear. In this paper, we exclude this case and limit ourselves to conditions where the flow properties vary sinusoidally in time. The amplitude

† Kistler, Type 410A. Natural frequency ≈ 40 kHz.

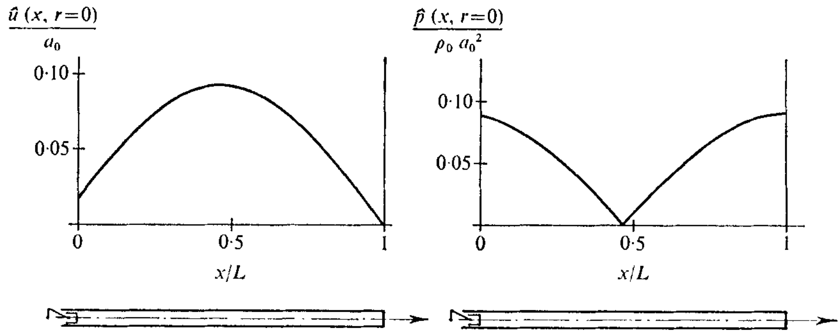

FIGURE 3. Amplitudes of the axial velocity and pressure on the tube axis. L = 1·4 m, l = 13·8 mm, tube radius R = 9·5 mm, f = 115 Hz, f_{res} = 122·4 Hz (air at $p_0 = 10^5 \mathrm{N/m^2}$ and T_0 = 298 °K).

of the pressure and of the axial velocity on the tube axis for such a case are shown in figure 3; see Merkli & Thomann (1975).

As the boundary layers were very thin in our investigation, the hot wire† had to be positioned near the tube wall to detect turbulence properly (see figure 1*a*). The long supports of the wire led to a relatively large volume of air in the wall, which had to be filled with wax, preventing further radial movement of the wire. As the resonance tube used for the hot-wire experiments consisted of interchangeable sections of different length it was possible to change the position x_{hw} of the hot wire by using different combinations of these tube elements.

For the flow visualization a plane of light through the axis of the Plexiglas tube was used (see figure 2). The plane was illuminated by a stroboscope (G. R. Strobolume 1540) synchronized with the piston motion. Because of light scattering and of a slight divergence of the light plane, the pictures are more informative on the right-hand than on the left-hand side of the tube. The main problem with the observations was avoiding any direct reflexion of light from the tube walls. For this purpose, the inner wall of the tube had to be partially painted black. As the flow is very sensitive to small disturbances, the smoke inlet was designed such that it could be sealed when not in use as shown in figure 1 (*b*). Normal cigarette smoke was used.

3. Hot-wire measurements

With the hot-wire probe frequencies at which turbulent bursts occurred at a fixed position x_{hw} were determined. Results for the standard tube are plotted in figure 4, where some theoretical lines A = constant are also shown. We see that the occurrence of turbulence closely follows these lines, yet the critical values of A are not the same below and above resonance. In a second set of experiments, the first occurrence of turbulence at the location $\hat{u} = \hat{u}_{max}$ was observed for different tube lengths. The results together with the theoretical lines $\hat{u}_{max} = \hat{u}_{max}(f)$ and A = constant are shown in figure 5. We see immediately that the experiments

† DISA, Type 55 A 01. Wire diameter = 5×10^{-6} m, wire length ≈ 1·2 mm.

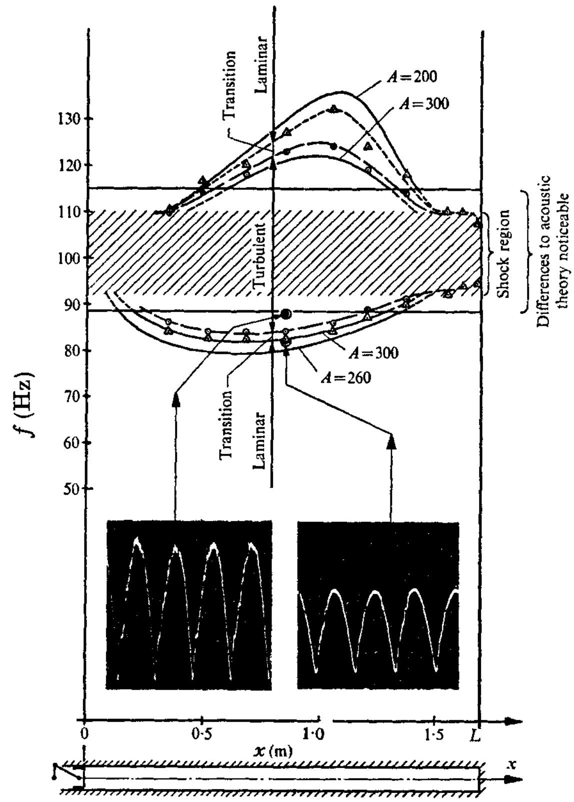

FIGURE 4. Observation of turbulence for some frequencies around resonance (standard tube). Measurements: △, first appearance of turbulent bursts; ○, regular and definite turbulent bursts.

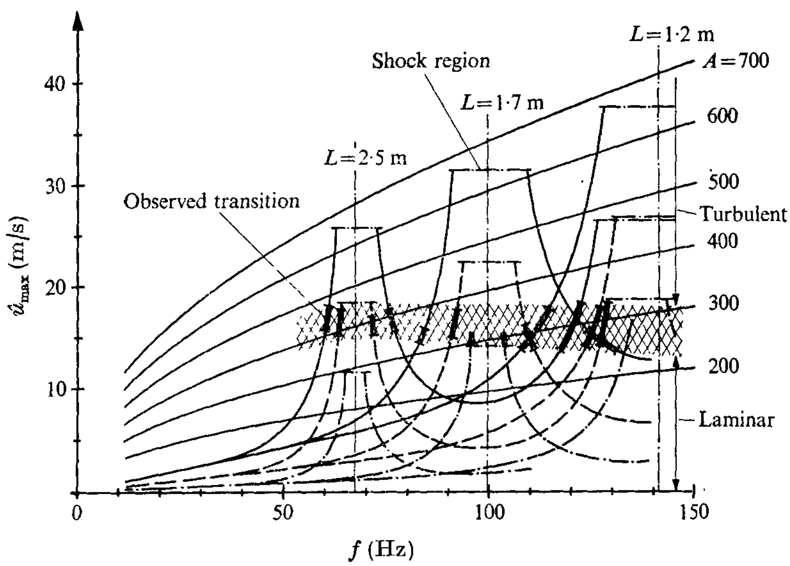

FIGURE 5. Observed transition at the location of $\hat{u}_{max}$ for different tube lengths L and piston amplitudes l (hot-wire measurements). ——, l = 13·8 mm; — — —, l = 7·1 mm; —·—, l = 2·85 mm.

do not confirm our expectation that transition is governed by A alone. The cause is the flow disturbance due to the hot-wire probe itself, as may be shown by flow visualization (see §4.2). As mentioned earlier, the geometry of the wire arrangement (in particular the distance y_{hw} from the hot wire to the tube wall) was the same for all experiments, but for different tube lengths, the frequency, and thus the boundary-layer thickness $\delta = O((\nu/\omega)^{\frac{1}{2}})$, was altered. A higher ω leads to a smaller δ and thus to a larger ratio y_{hw}/δ. This means that the relative flow disturbance due to the hot wire grows with increasing frequency, resulting in lower values of A_c. This corresponds to the finding in figure 4 that A_c below resonance (low frequency) is higher than A_c above resonance (higher frequency). As may be seen from figure 5, it was possible to observe the transition in the second resonance for a tube length of $L = 2{\cdot}5$ m. Also these results agree very well with the general trend shown in this figure. However, the flow disturbance due to the hot wire does not make these results useless, especially as the order of magnitude of A_c (although not constant) is supported by the visual observations. They provide us with some valuable details about turbulence.

(*a*) In no case was turbulence observed during a whole cycle in spite of the measuring probe disturbing the flow. There were turbulent bursts around the velocity peaks but these were always followed by relaminarization as illustrated by the hot-wire signals in figure 4. (These two recordings have the same scale and were linearized. As the hot-wire measurements cannot indicate the flow direction, the signals are rectified sine waves.) The details of the turbulent flow described above might provide the explanation for the discrepancies between experiments and the stability theory of von Kerczek (1973), see §5.

(*b*) The observed value of $A_c(x)$ in figure 4 might be changed by the gradients dp/dx and $\partial u/\partial x$ and by spreading of turbulence from regions with $A > A_c$ locally to subcritical regions. As the observed $A_c(x)$ is constant, these effects are negligible or cancel each other.

(*c*) For harmonic motion of the gas, with $u(x, r) \rightarrow 0$ for $x \rightarrow L$ (therefore $A \rightarrow 0$), there were always sections with fully laminar flow towards the tube ends. However, it was not possible in our experiments to reach values of A much larger than A_c (see figure 5), as we were limited by the fundamental change in the flow due to the shock waves in the frequency band near resonance (see Chester 1964†).

(*d*) Outside the shock region, where nonlinear effects already occur, no influence of these on A_c (based on linearized theory) was noted. This may be seen from figure 4 and especially from figure 5, where, for different experiments, the same values of A_c are found independently of how near the transition region lies to the shock region.

(*e*) For very small piston amplitudes, turbulence does not occur at all, and for slightly larger amplitudes, appears in the shock region only.

† The largest value A_{max} of A is reached at the lower shock-region boundary of the first resonance (see figure 5). A good estimate of A_{max} may be calculated by using a simplified criterion for the shock-boundary frequency and a simple acoustic wave theory (see Merkli 1973):

$$A_{max} \approx \left(\frac{a_0 l}{\pi\nu(\gamma+1)}\right)^{\frac{1}{2}} \left[\pi + \left((\gamma+1)\frac{l}{L}\right)^{\frac{1}{2}}\right],$$

where a_0 = speed of sound, l = piston amplitude and L = tube length.

4. Flow-visualization experiments

4.1. *The vortex patterns*

Figure 6 (plate 1) shows a smoke pattern found in the tube. It was illuminated by the stroboscope synchronized to the motion of the piston. A number of vortices along the tube wall can be observed. As the mechanism of this phenomenon is not yet understood, only observations are presented here.

As long as the flow is laminar, the vortices persist for an unlimited time, while artificially generated disturbances of the flow (smoke injection) decay rapidly. Therefore, it was possible to put together figure 6 from two exposures, taken one after the other but at the same phase of the periodic motion. The vortex pattern is convected periodically with the acoustic motion, but the visual effect can be suppressed by synchronizing the stroboscope with the piston motion. As the vortices persist in time and can even be reproduced at the same place in different experiments, they may be caused by a small waviness or roughness of the tube wall. Much care was taken to keep the Plexiglas surface as smooth as possible but vortices were always observed. It was not possible, therefore, to determine whether vortices would be formed on a 'perfect' wall too.†

The vortices are outside the normal boundary layer, in the region of the radial change of sign of the acoustic streaming (see Rayleigh 1965, p. 342), and their sense of rotation corresponds to this secondary flow. Often the vortices have the form of vortex rings. This can be seen clearly from figure 6 as the light plane cuts such a vortex ring twice, on the right and left side of the tube. The eddies, being weak, cannot be discerned from normal pressure or hot-wire measurements along the tube. Similar vortices were noted in oscillating liquid columns by Pélissier (1973). If turbulence or shocks occurred, no eddies could be observed as the smoke diffused too quickly.

4.2. *The transition to turbulence*

The laminar boundary layer itself, which had a thickness $\delta \approx 3(\nu/\omega)^{\frac{1}{2}} \approx 0{\cdot}5\,\text{mm}$, was too thin to allow the observation of turbulence directly. Yet with turbulence within the Stokes layer, the aforementioned vortices become irregular and the smoke spreads diffusively in the tube. Therefore, it was possible to determine the onset of turbulence with good accuracy by direct observation of the vortices. Figures 7–10 (plates 2 and 3) show such transition sequences for the standard tube. Each figure contains 5 exposures taken at the same phase of a cycle, but each 2 s apart. While for a frequency of $f = 84{\cdot}0\,\text{Hz}$ essentially no change from one exposure to the next is noticeable, some changes can be seen for $f = 86{\cdot}1\,\text{Hz}$, changes are evident for $f = 88{\cdot}3\,\text{Hz}$ and become even stronger for $f = 90{\cdot}1\,\text{Hz}$ (shocks occur in this experiment for $f > 93\,\text{Hz}$ only). The transitions were assumed to take place for $f_{tr} = 86$–88 Hz, compared with $f_{tr} = 82$–84 Hz measured with the hot wire (figures 4 and 5). This reflects the disturbance of the flow by the hot-wire probe, which is quite small for frequencies near resonance for the standard tube, becomes larger for higher frequencies and vanishes for lower ones.

† Measurements of the actual tube surface show a large-scale waviness with wavelengths of 80–200 mm and amplitudes of 10 μm and small-scale waves irregularly superimposed with wavelengths of order 1 mm and amplitudes smaller than 1 μm.

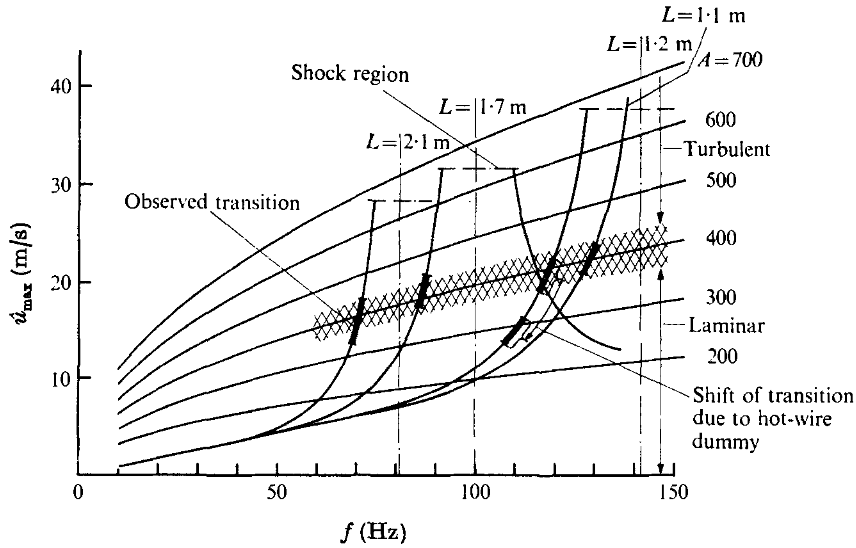

FIGURE 11. Observed transition for different tube lengths according to visual observations (l = 13·8 mm, R = 9·5 mm).

With the smoke method, the transition was observed for other tube lengths too. The results are shown in figure 11. We now find confirmation that the occurrence of turbulence is characterized by the local Reynolds number A or Re_δ and different experiments yield the same critical value of approximately $A_c = 400$. To prove our suggestion that the hot-wire probe disturbs the flow, the transition was also observed using the smoke method with a hot-wire dummy mounted as in the experiments described in §3. Its influence is shown in figure 11 for the case L = 1·2 m. The same region of transition is found as with the hot-wire measurements, thus confirming the statement made earlier.

5. Conclusions

Transition in a Stokes layer has been investigated experimentally and a critical Reynolds number $A_c \approx 400$ found. This result is in fair agreement with other observations: $A_c = 800$ (Li 1954), $A_c = 160$ (Vincent 1967), $A_c = 230$ (Collins 1963), $A_c = 700$ (Sergeev 1966), A_c = 150–420 (Pélissier 1973) and $A_c = 730$ (Daneshyar). All experimental values have the same order of magnitude. The scatter of the data probably reflects the usual sensitivity of transition to small effects, different in every experiment. This does not mean that the same experiment is not reproducible. On the contrary, we found the occurrence of transition to be very well fixed. Moreover, there is little room for individual interpretation of what is turbulent flow, as may be seen from the marked change in the flow in figures 4 or 7–10.

We did not observe any case in which turbulence occurred throughout a whole cycle. However, owing to the shocks arising in a frequency band around resonance, we could not reach conditions where $A \gg A_c$ (see figure 5). As indicated by a rough estimate (Merkli 1973), it might be possible that even for large values of A the fully turbulent Stokes layer does not exist but an experimental confirmation is still lacking.

Von Kerczek (1973) mentioned some results of a quasi-steady stability theory. According to this theory, turbulence in a Stokes layer must occur for $A > 865$ and is impossible for $A < 120$. This statement is confirmed by all experiments known (see above). The main part of von Kerczek's (1973) paper, the linear stability theory, indicates absence of turbulence at much higher Reynolds numbers. It is based on the criterion that a small disturbance should show a net increase over one full cycle. This criterion is too restrictive as, according to our observations, a disturbance may grow, lead to turbulent bursts and decay by relaminarization in the same period.

REFERENCES

Chester, W. 1964 Resonant oscillations in closed tubes. *J. Fluid Mech.* **18**, 44.

Collins, J. I. 1963 *J. Geophys. Res.* **18**, 6007.

Kerczek, C. von 1973 On the stability of Stokes layers. Ph.D. thesis, The Johns Hopkins University, Baltimore, Maryland.

Kerczek, C. von & Davis, S. H. 1972 The stability of oscillatory Stokes layers. *Studies in Appl. Math.* **2**, 239.

Li, H. 1954 *Beach Erosion Board, U.S. Army Corps of Engineers, Washington, D.C., Tech. Memo.* no. 47.

Merkli, P. 1973 Theoretische und experimentelle thermoakustische Untersuchungen am kolbengetriebenen Resonanzrohr. Dissertation, Eidgenössische Technische Hochschule, Zürich, no. 5151.

Merkli, P. & Thomann, H. 1975 Thermoacoustic effects in a resonance tube. *J. Fluid Mech.* (to appear).

Pélissier, T. 1973 Mouvement pseudo-périodique d'une colonne liquide, critères de transition. Thesis, Université de Provence. (See also *C.N.R.S. Rep.* A 0 7780.)

Rayleigh, Lord 1965 *Theory of Sound*, vol. 2. Macmillan.

Sergeev, S. I. 1966 Fluid oscillations in pipes at moderate *Re*-numbers. *Fluid Dyn.* **1**, 121.

Vincent, G. E. 1957 *Proc. Conf. Coastal Engng*, vol. 16. University of Florida.

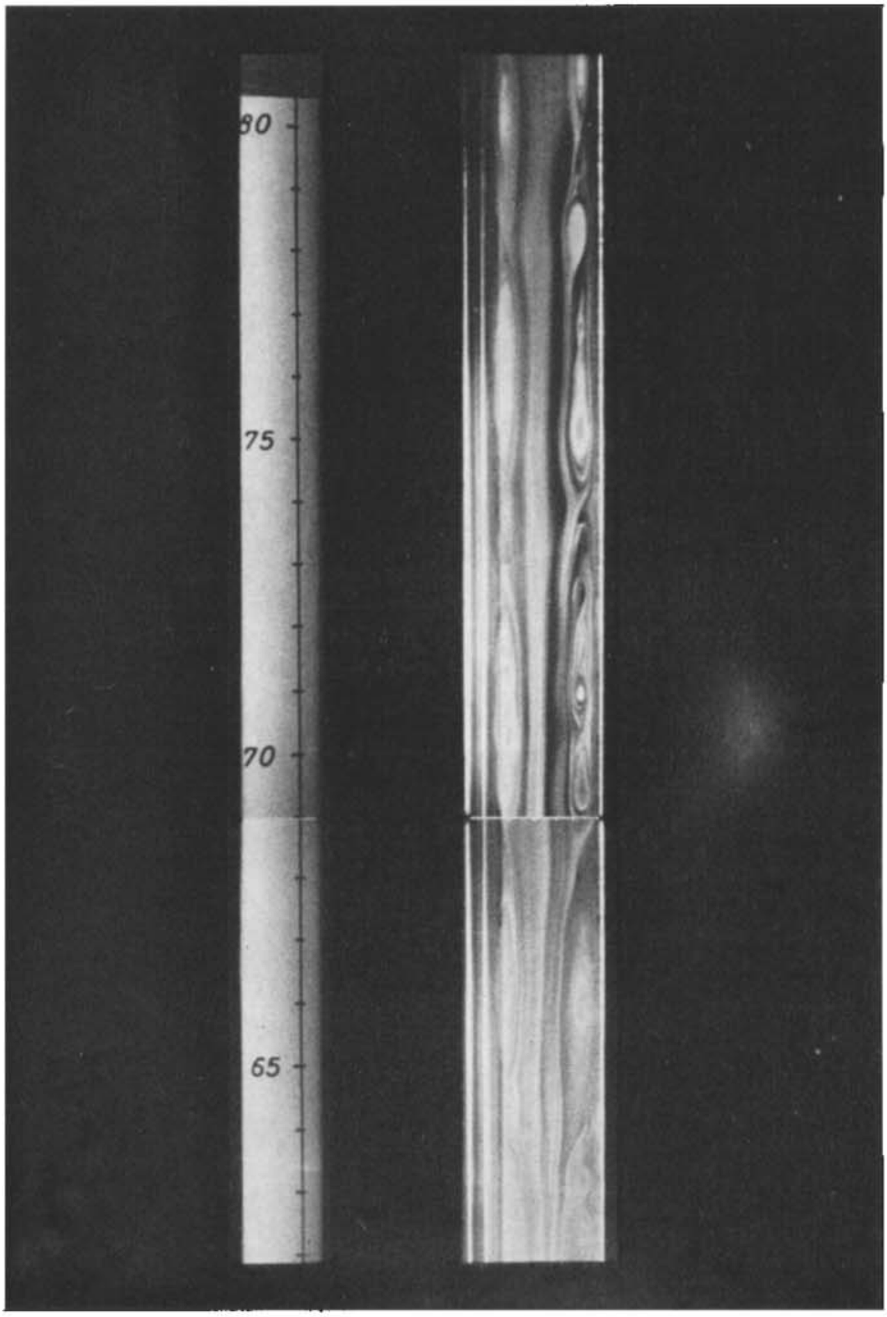

FIGURE 6. Vortex pattern at $f = 60{\cdot}2$ Hz in the standard tube characterized by the following values: $L = 1{\cdot}7$ m, $l = 13{\cdot}8$ mm, $R = 9{\cdot}5$ mm, $f_{res} \approx 100$ Hz (air at $p_0 = 10^5\,\mathrm{N/m^2}$ and $T_0 = 298$ °K). Scale on left-hand side gives distance x from piston in cm.

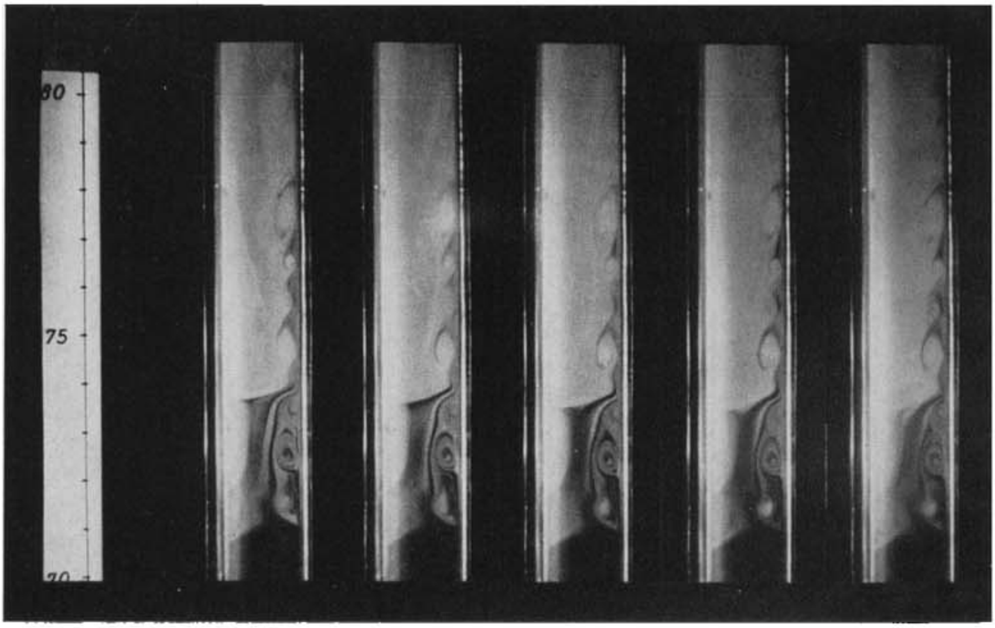

FIGURE 7. Sequence of exposures taken at intervals of 2 s. $f = 84{\cdot}0$ Hz, $f_{res} \approx 100$ Hz, standard tube.

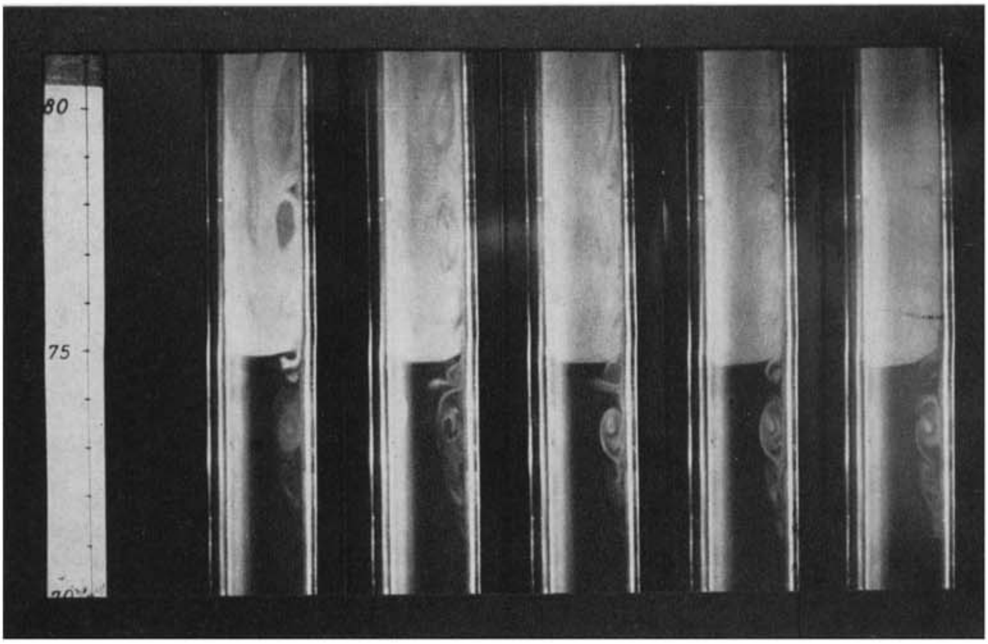

FIGURE 8. Sequence of exposures taken at intervals of 2 s. $f = 86{\cdot}1$ Hz, $f_{res} \approx 100$ Hz, standard tube.

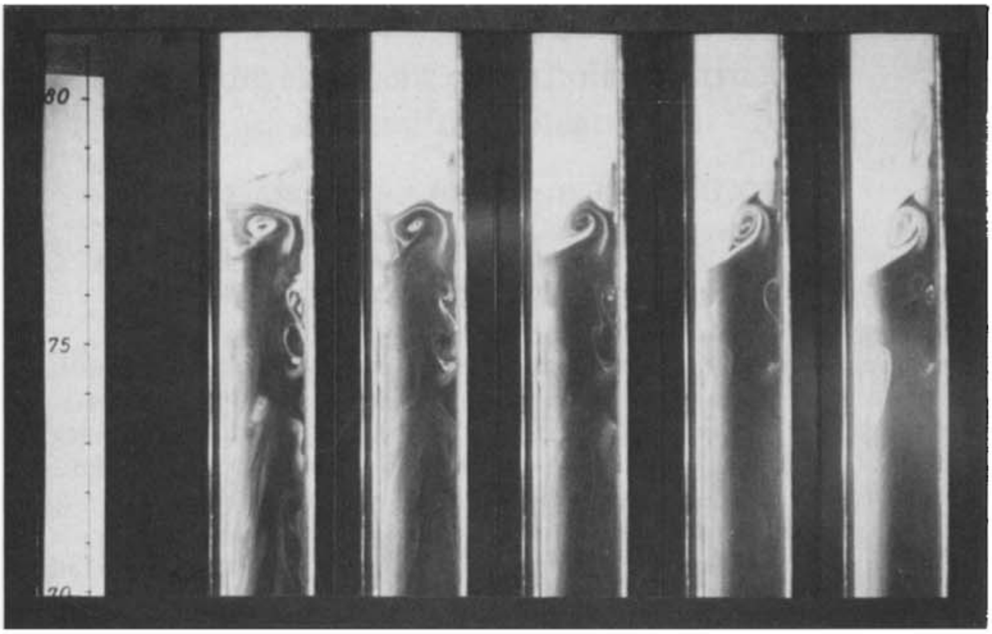

FIGURE 9. Sequence of exposures taken at intervals of 2 s.
$f = 88{\cdot}3$ Hz, $f_{res} \approx 100$ Hz, standard tube.

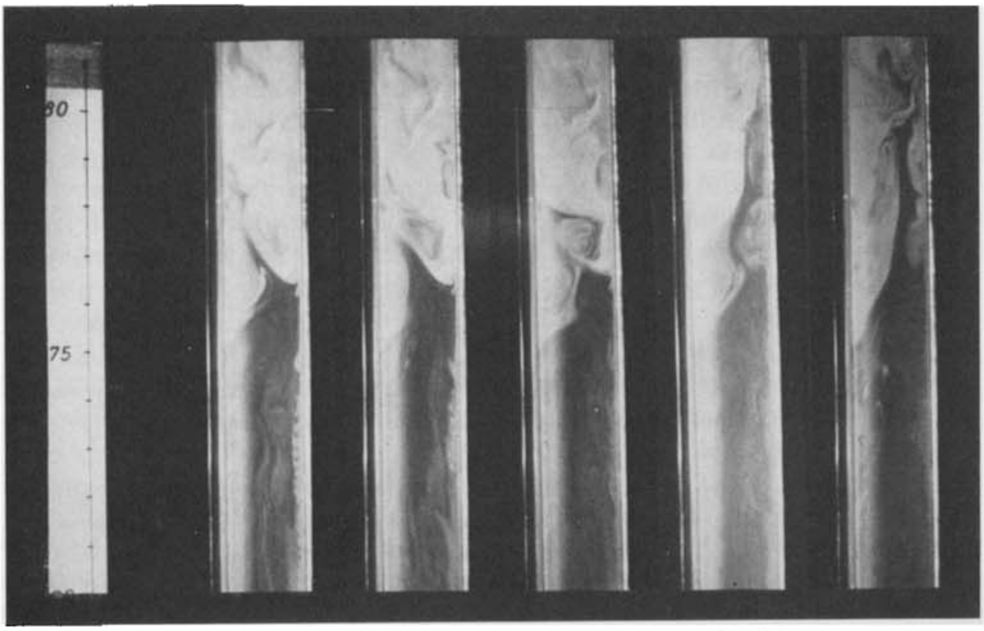

FIGURE 10. Sequence of exposures taken at intervals of 2 s
$f = 90{\cdot}1$ Hz, $f_{res} \approx 100$ Hz, standard tube.